

UCLA

UCLA Previously Published Works

Title

Thermo-economic analysis of a solid oxide fuel cell-gas turbine hybrid with commercial off-the-shelf gas turbine

Permalink

<https://escholarship.org/uc/item/0gg32846>

Authors

Rosner, Fabian

Samuelsen, Scott

Publication Date

2022-10-01

DOI

10.1016/j.apenergy.2022.119745

Copyright Information

This work is made available under the terms of a Creative Commons Attribution License, available at <https://creativecommons.org/licenses/by/4.0/>

Peer reviewed



Thermo-economic analysis of a solid oxide fuel cell-gas turbine hybrid with commercial off-the-shelf gas turbine

Fabian Rosner^{a,b,*}, Scott Samuelsen^b

^a Advanced Power and Energy Program, University of California, Irvine, CA 92697-3550, USA

^b Sustainable Energy Systems Group, Energy Analysis and Environmental Impacts Division Lawrence Berkeley National Lab, 1 Cyclotron Road, Berkeley, CA 94720, USA

HIGHLIGHTS

- Integration of off-the-shelf GT into SOFC-GT hybrid.
- Comparison of constant spool speed, variable spool speed and VIGV operation.
- Investigation of surge margin.
- Thermodynamic and economic performance evaluation.

ARTICLE INFO

Keywords:

Solid oxide fuel cell
SOFC-GT hybrid
Techno-economics
Economic optimization
Off-the-shelf gas turbine

ABSTRACT

The thermodynamic and economic performance of a natural gas-fueled solid oxide fuel cell (SOFC)-gas turbine (GT) hybrid system with a commercial off-the-shelf GT is investigated. Until today, commercial GTs are primarily engineered for the direct use of energy dense fuels, such as natural gas, and the integration of commercial GTs into a SOFC-GT hybrid remains challenging. In this work technically feasible and economically viable GT operating modes are identified to gauge the technology's competitiveness on the free market. Steady state, full load operating conditions were established for various GT operating modes: I) constant spool speed operation, II) variable spool speed operation and III) partially closed compressor inlet guide vanes. For each GT operating mode, the performance was investigated over a range of SOFC fuel utilization factors, while considering physical constraints inside the SOFC, such as local temperature gradients in flow direction as well as overall cell temperature differences. The results of the thermodynamic evaluation served as inputs for the economic analysis of the SOFC-GT hybrid power plant. The results show that the integration of an off-the-shelf GT not only results in a significant derating of the GT, but also substantially impacts the SOFC operation, the main power producer in this SOFC-GT hybrid. To maximize the SOFC power output it is desirable operate the GT in a region of high air mass flow rates and low pressure ratios, which increases the number of stacks that can be accommodated and reduces the SOFC cooling requirement. The lowest costs of electricity are obtained at constant spool speed operation, while the highest efficiencies are reached at variable spool speed operation. Critical for the integration of off-the-shelf GTs, which historically have been designed for natural gas, is the surge margin. The largest surge margins are obtained by closing the compressor inlet guide vanes. Furthermore, higher SOFC fuel utilization factors are shown to increase the surge margin as the turbine firing temperature is decreased.

1. Introduction

With current operating practices used in the power sector, it is not possible to maintain the sensitive ecological balance of the earth's ecosystems. The steady increase of greenhouse gasses in the atmosphere

related to the use of fossil fuels together with the emission of criteria pollutants lead to environmental degradation and changes in rainfall and weather patterns. To diminish the environmental footprint of the power sector, highly efficient and environmentally sensitive energy conversion systems are of major importance. When utilizing fossil hydrocarbon fuels, the thermal efficiency directly translates to slower

* Corresponding author at: Sustainable Energy Systems Group, Energy Analysis and Environmental Impacts Division Lawrence Berkeley National Lab, 1 Cyclotron Road, Berkeley, CA 94720, USA.

E-mail addresses: fmr@apep.uci.edu, fabianrosner@lbl.gov (F. Rosner).

<https://doi.org/10.1016/j.apenergy.2022.119745>

Received 1 October 2021; Received in revised form 21 June 2022; Accepted 23 July 2022

Available online 26 August 2022

0306-2619/© 2022 The Authors. Published by Elsevier Ltd. This is an open access article under the CC BY license (<http://creativecommons.org/licenses/by/4.0/>).

Nomenclature

Symbols

a	Activity, in –
a, b, c	GT Map Scaling Parameter, in –
AER	Annual Escalation Rate, in –
CCF	Capital Charge Factor, in –
CF	Capacity Factor, in –
COE	First Year Levelized Cost of Electricity, in \$/MWh
E	Cell Potential, in V
F	Faraday Constant, 96,485C/mol
\dot{m}	Mass Flow, in kg/s
MWH	Annual Net-Power Gen. at 100 % Capacity, in MWh
n	Number of Electrons Participating in the Electrochemical Reaction, in –
OC	Annual Operating Cost, in \$
p	Pressure, in bar
PR	Pressure Ratio, in –
R	Universal Gas Constant, 8.314 J/mol/K,
RC	Reference Cost, in \$
RY	Reference Year, in –
\hat{s}_{rxn}	Reaction Entropy, in J/mol/K
SC	Scaled Cost, in \$
SM	Surge Margin, in %
SY	Scaled/Projected Year, in –
T	Temperature, in K,
TOC	Total Overnight Capital, in \$
V_{SOFC}	Operating Voltage of the Fuel Cell, in V
y	Mole Fraction, in –

$\Delta\alpha_{VIGV}$	VIGV Closing Angle, in degrees
ν_i	Stoichiometric Coefficient, in –
η	Efficiency, in –
η_{act}	Activation Loss, in V
η_{ohmic}	Ohmic Loss, in V
η_{conc}	Concentration Loss, in V

Superscripts

0	Standard State
ν	Stoichiometric Coefficient

Subscripts

0	Standard State
act	Activation Overpotential
conc	Concentration Overpotential
Corr	Corrected
Norm	Normalized
ohmic	Ohmic Overpotential
OP	Operating Point
R	Reference
rxn	Reaction

Abbreviations

COE	Cost of Electricity
FU	Fuel Utilization
GT	Gas Turbine
LHV	Lower Heating Value
SOFC	Solid Oxide Fuel Cell
TIT	Turbine Inlet Temperature
VIGV	Variable Inlet Guide Vane

resource depletion and lower carbon emissions. Solid oxide fuel cell (SOFC)-gas turbine (GT) hybrid systems have shown to reach exceptional efficiencies with fuel-to-energy conversion values of greater than 75 %-LHV [1–3]. While SOFC-GT hybrid systems can operate on natural gas during a transition period, they can also be operated on carbon free H₂ generated from renewable resources [4]. The ability of reaching very high efficiencies and being able to operate on natural gas as well as H₂ uniquely positions SOFC-GT hybrid systems as an important key technology for the energy infrastructure of the future.

In an SOFC-GT hybrid, most of the fuel is converted to electricity via highly efficient electrochemical reactions. This chemistry precludes the formation of pollutants, and consequently, SOFC-GT hybrids emit virtually no criteria pollutants.

Over the years substantial efforts have been undertaken to study SOFC-GT hybrid systems in more detail. An SOFC-GT hybrid system with steam injection into the natural gas and without anode off-gas recirculation was studied by Chan et al. [5,6] focusing on the effects of pressure variation and fuel flow rate. In a similar system, Calise et al. [7] performed an exergy analysis and identified the SOFC as the largest source of exergy destruction despite its high efficiency. Similarly, Haseli et al. [8] concluded that exergy destruction mostly originates from the SOFC and combustor, whereby, it is desirable to convert most of the fuel in the SOFC even if that leads to a lower firing temperature and turbine efficiency. In the work of Eisavi et al. [9], exergy destruction was found to occur predominantly in the after burner and SOFC. Additionally, different stack configurations were investigated and a serial air flow in combination with parallel fuel injection was found to be advantageous despite the higher pressure drop. A considerable amount of research work in literature focuses on operational aspects of the SOFC, such as carbon deposition or thermal gradients. Carbon deposition inside the

SOFC leads to catalyst deactivation and has been analyzed in the context of varying steam to carbon ratios and their impact on the plant performance [10] as well as in the context of gas stability [11]. Uechi et al. [12] conducted research on a system with anode off-gas recycle and external reformer, which is thermally coupled with the SOFC, looking at turbine inlet temperatures, pressure ratios, ambient temperatures and steam to carbon ratios. Also Yang et al. [13] studied hybrid cycles, similar to the ones aforementioned, investigating fuel cell operating temperatures for systems with internal or external reformer. Thermal gradients within the ceramic electrolyte membrane have been investigated via 1D models, which take heat and mass transfer phenomena inside the cell into account. Wongchanapai et al. [11] studied the effects of pressure ratio, TIT and internal temperature gradients in a direct biogas SOFC hybrid system and identified strong thermal gradients at the cell inlet due to the endothermic reforming reaction. Cuneo et al. [14] investigated the impact of cell degradation on the temperature profile and Zhang et al. [15] studied thermal cell gradients during load transients. A study conducted by Wu et al. [16] focuses on strategies to better control thermal gradients during SOFC operation. An optimization study conducted by Shirazi et al. [17] optimized an SOFC-GT hybrid system with GT exhaust recuperation and anode off-gas recycle. The economic analysis revealed that the lowest cost was achieved at a pressure ratio of 7.1, a fuel utilization factor of 0.79 and an operating voltage of 0.628 V.

Aspects of GT integration into an SOFC-GT hybrid have been studied to a lesser extent. Historically, commercially offered GTs have been engineered for energy dense fuels such as natural gas. The utilization of lower heating value fuels (e.g. the anode off-gas from an SOFC) can result in a flow mismatch between the GT compressor and GT expander. This issue is eliminated and ignored with the use of custom-engineered

GTs, an approach which is often adopted in simulation work concerned with the evaluation of the full thermodynamic potential of a technology [18,19]. However, GT vendors are not expected to offer GTs specifically designed for SOFC-GT hybrid applications. Thus, engineers will need to rely on current GT offerings for the design of SOFC-GT hybrid systems.

In this context, Lundberg et al. [20] investigated the integration of an SOFC into a Mercury 50 GT looking at configurations without a bottoming cycle and configurations with bottoming steam and ammonia Rankine cycles. The GT was simulated at its design point condition with constant geometry. Only minor design modifications were necessary to accommodate the fuel cell. The inlet stators were adjusted, the air inlets to the combustion chamber were resized due to the higher inlet temperature and the combustor main case has been redesigned using high temperature materials. Park et al. [21] integrated an SOFC into a fixed geometry micro GT and found a significant reduction of the GT power generation compared to the design point. The GT power output can be increased by increasing the operating temperature of the SOFC; however, this requires the GT to operate close to the compressor surge line. Costamagna et al. [22] conducted simulations on the integration of an SOFC into a micro turbine using compressor performance parameters and found that even for very small systems of 300 kW, efficiencies of greater than 61 % LHV are possible. Furthermore, variable speed operation was shown to be superior to constant speed operation under part load conditions. The works of Barelli et al. [23] and Kimijina and Kagsagi [24] showed that, under part load, the efficiency can be maintained at a very high level when using variable speed control for the GT. Calise et al. [25] investigated a similar plant design with anode off-gas recirculation under part load at constant speed, and suggest that for part load operation the fuel to air ratio should be kept constant to obtain higher efficiencies. A similar system was studied by Campanari [26] under part load conditions who came to the same conclusion and additionally showed that variable speed operation of the GT is advantageous (with respect to efficiency) under varying ambient conditions. The economic impact of these varying GT operating conditions however remains unexplored.

In summary, various SOFC-GT hybrid systems have been studied in literature; however, key aspects of the integration of commercial GTs into an SOFC-GT hybrid are not fully addressed. While variable speed operation has been found to be favorable with respect to efficiency under part load conditions, it is not clear how variable speed operation impacts full load operation, surge margin, and economics. This study aims to close this gap in the literature and provides novel insights to better understand the derating effects of commercial GTs operating under SOFC-GT hybrid conditions by comparing three GT operating modes, I) constant speed, II) variable speed and III) variable inlet guide vanes (VIGV) over a range of fuel utilization factors by the means of surge margin, power output, efficiency, specific cost and cost of electricity (COE).

2. Methodology

This work is building upon previous studies conducted by the authors, which include the optimization of the SOFC cell design with respect to thermal gradients and specific cell cost under SOFC-GT hybrid operating conditions [27] and the optimization of the SOFC-GT hybrid system design while considering thermal limitations within the SOFC [18]. The results suggest that it is favorable to operate the hybrid system at a pressure ratio of approximately 5 bar and that the operating point of the GT is rather unconventional when compared to commercial GTs due to the high air requirement of the SOFC, which determines the size of the GT rather than the GT's power output. Thus, to reach a plant scale of 10 MW, a GT of approximately 1.6 MW (ISO rating) is needed to meet the cooling demand of the SOFC. After comparing various commercial GT models, a Dresser Rand KG2-3G EF with an ISO rating of 1.83 MW has been selected for this work (more details on the GT selection are discussed later). To facilitate a fair comparison between earlier results and

this work, fundamental design features of the hybrid system and performance metrics are kept consistent with previous work. In this work, three GT operating modes I) constant speed, II) variable speed and III) VIGV are evaluated under full load operating conditions for various fuel utilization factors at steady state. The SOFC underlies thermal constraints consistent with previous work. In this work, the GT is a commercial GT that operates on a compressor map and turbine map. The steady state simulations are carried out using a well-established commercial chemical process simulation software that contains built-in libraries for chemical compounds as well as thermodynamic models. Together with external software packages for heat exchanger design and rating, and custom models, the performance of the system is evaluated. The thermodynamic and rate-based kinetic results, such as heat exchanger surface areas, obtained from the simulation serve as basis for equipment sizing and the economic evaluation.

2.1. Design basis

2.1.1. Fuel characteristics

The SOFC-GT hybrid systems studied in this work use natural gas. Natural gas can be internally reformed inside the SOFC producing H_2 and CO. Carbon monoxide typically undergoes further conversion via the water gas shift reaction producing additional H_2 . While CO can be oxidized electrochemically inside the SOFC, it is almost exclusively H_2 that reacts inside the SOFC due to kinetic limitations. The reforming reaction is of endothermic nature and can provide cooling to the SOFC. Natural gas compositions can vary, in this work an average gas composition representative for the U.S. is used [28]. Modifications have been made to account for trace components in accordance with [29]. The detailed composition is provided in Table 1. The natural gas supply pressure is assumed to be 4.1 bar.

Table 1
Natural gas composition.

Component	Mole-%
Methane	93.08746
Ethane	3.19957
Propane	0.69991
<i>n</i> -Butane	0.39995
Carbon Dioxide	0.99987
Nitrogen	1.59978
Water	0.00329
Oxygen	0.01000
Hydrogen Sulfide	0.00004
<i>Tert</i> -Butyl Mercaptan	0.00013

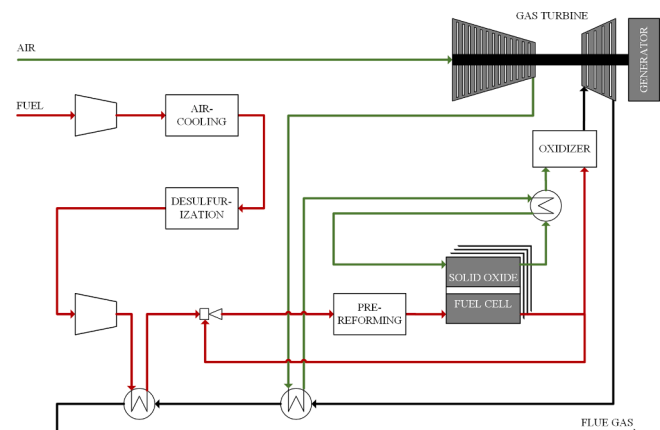


Fig. 1. Solid oxide fuel cell - gas turbine hybrid configuration [18].

2.1.2. Solid oxide fuel cell hybrid configuration

In an SOFC-GT hybrid, a GT is used to pressurize the SOFC while serving as the “bottoming cycle.” Higher operating pressures allow the SOFC to reach higher fuel utilizations (FU), higher operating voltages and higher current densities. Moreover, high quality heat generated in the fuel cell itself can be exploited together with heat generated from unutilized fuel in the expander section of the GT. This synergy between the SOFC and GT allows the SOFC-GT hybrid to reach extremely high efficiencies. In this work, the same configuration as in [18] has been chosen to allow direct comparisons between the optimized case in [18] using a custom-designed GT and results from this work using a commercial off-the-shelf GT. In this design, an ejector recycles a portion of the anode off-gas back to the pre-reformer to avoid carbon deposition. The amount of gas recycle is established based on gas phase stability considerations [30]. Additionally, the anode recycle provides heat for fuel preheating. On the cathode side, the GT exhaust gas is utilized to pre-heat the incoming air from the compressor. In order to reach the necessary SOFC inlet temperature of 700 °C, a high temperature recuperator is used. Due to the extreme operating conditions and low pressure drop requirements modern high temperature alloys and novel low pressure drop designs are essential [31]. A flow sheet of the plant design is provided in Fig. 1. Ambient conditions correspond to ISO conditions of 1.013 bar and 15 °C. Air composition is provided in [18].

2.2. Power block modelling

2.2.1. Ejector

As mentioned before, an ejector is used to recycle a portion of the anode off-gas back to the pre-reformer. Ejectors are static devices that use a high-pressure stream to compress a lower pressure stream. The use of an ejector is advantageous in SOFC applications as the hot recycle stream does not have to be cooled prior to the ejector opposed to when using a compressor. Furthermore, equipment cost and maintenance costs for ejectors are very low. In this work a 2-dimensional ejector model developed by Zhu et al. [32] has been employed which accounts for the velocity profile in the suction chamber. This model has been specifically developed for SOFC anode off-gas recirculation applications where the secondary flow is much larger and the pressure increase smaller than in typical ejector applications. In accordance with [32], the ejector is sized for each study scenario individually to operate at its respective design point and accommodate the necessary recycle in order to avoid carbon deposition.

2.2.2. Pre-reformer

Before the CH₄-rich fuel gas is introduced into the SOFC, 20 % of the CH₄ is pre-reformed in an external pre-reformer. The pre-reformer is integrated into the SOFC furnace in a fashion that allows for radiation heat transfer between the SOFC stack and the pre-reformer. The thermal integration in this design is similar to the design described in [33]. Under these conditions, the reforming reactions can be either limited by the quantity of catalyst present or the heat transfer from the SOFC to the pre-reformer. The purpose of the pre-reformer is to pre-reform higher hydrocarbons, which are present in low concentrations and pose a risk of carbon deposition. Only limited CH₄-conversion is desirable in the pre-reformer, which can reduce thermal gradients inside the SOFC, in order to take advantage of internal reforming.

2.2.3. SOFC

The SOFC is modelled as a planar, anode supported cell with anode and cathode streams flowing in co-flow. The model utilizes the Nernst equation for the reaction between H₂ and O₂. Although CO can react electrochemically in SOFCs, the kinetics are sufficiently slow compared to the dominant H₂ reaction that it can be neglected. Therefore, CO is rather shifted to CO₂ producing H₂ than electrochemically oxidized. The reforming reaction rate is based upon kinetic expressions, whereas the water gas shift reaction is considered to quickly reach equilibrium.

Table 2

Summary of internal reforming solid oxide fuel cell and gas turbine parameters.

SOFC Geometry	Value	Unit
Fuel/Air Channel Length	0.2	m
Fuel/Air Channel Width	0.002	m
Rib Width	0.003	m
Number of Channels	50	–
Fuel Channel Height	0.001	m
Air Channel Height	0.002	m
Interconnect Height	1500	μm
Anode Thickness	400	μm
Electrolyte Thickness	8	μm
Cathode Thickness	20	μm
SOFC Operational Parameters	Value	Unit
Operating Pressure	~7	bar
Operating Voltage	0.82	V
Inlet Temperature Anode	973.15	K
Inlet Temperature Cathode	973.15	K
Max. local PEN Temp. Gradient	15	K/cm
Overall PEN Temp. Difference	150	K
GT Operational Parameters (Design Point)	Value	Unit
Compressor Polytropic Efficiency	84.35	%
Expander Polytropic Efficiency	84.36	%
Compressor Mechanical Efficiency	98.03	%
Expander Mechanical Efficiency	98.03	%
Turbine Inlet Temperature	943.3	°C
Combustor Pressure Drop	3	%
Combustor Heat Loss	1	%-LHV

$$E_{\text{Nernst}} = \sum E_{\text{Half Reactions}}^0 + \frac{\Delta \hat{s}_{\text{rxn}}}{nF} (T - T_0) + \frac{RT}{nF} \ln \left(\frac{\prod a_{\text{Products}}^{v_i}}{\prod a_{\text{Reactants}}^{v_i}} \right) \quad (1)$$

Three major losses are accounted for, in order to obtain the real cell operating voltage.

$$V_{\text{SOFC}} = E_{\text{Nernst}} - \eta_{\text{act}} - \eta_{\text{ohmic}} - \eta_{\text{conc}} \quad (2)$$

Activation losses are based on the Butler-Volmer equation. Ohmic losses are calculated using Ohm's law and concentration losses are derived from the diffusion kinetics. More details on the SOFC model can be found in [34], nevertheless, a concise summary of the model's assumptions is provided below.

- Homogeneous compound distribution in finite control volume.
- Electrochemical oxidation of H₂ occurs at the anode-electrolyte interface, with the reaction kinetics controlled by the local PEN temperature.
- 100 % of the surface area under the interconnect rib is active for H₂ oxidation but inactive for CH₄ reformation.

The geometric cell design was established in previous work [27]. The cell geometrical parameters used in this work are summarized in Table 2. The electrolyte material is yttria stabilized zirconia which is typically used in a temperature range from 600 to 1000 °C and cell materials and geometric parameters are not changed throughout this study.

2.2.4. GT

To model the off-design performance of the commercial GT and evaluate the GT derating due to the hybridization, a detailed GT model has been developed based on normalized compressor and turbine maps. The GT selected in this work is a Dresser Rand KG2-3G EF, which is rated for 1.83 MW under ISO conditions using CH₄ as fuel [35]. With its design point compression ratio of 7:1 and mass flow rate of 9.48 kg/s [35], it is suitable for the integration into an SOFC-GT hybrid systems of approximately 10 MW, similar to [18]. The EF (externally fired) version of this GT will allow for an easier SOFC integration as compared to GTs where the combustor is integrated into the GT casing. Furthermore, Dresser Rand offers a Power Oxidizer with this model for the utilization of low heating value gases (the SOFC anode off-gas is a low heating value gas)

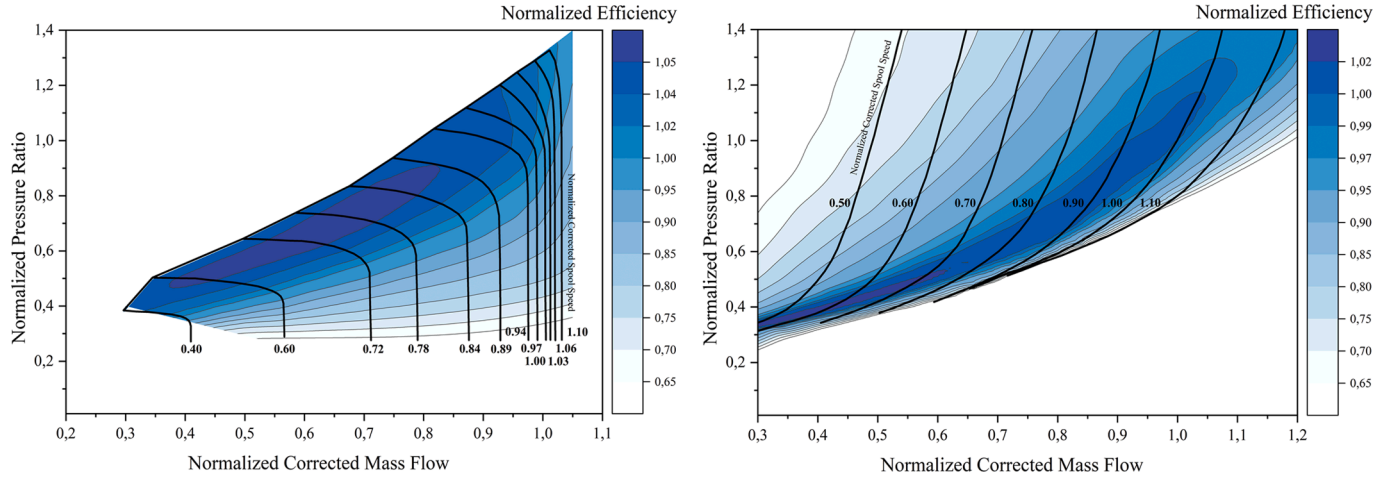


Fig. 2. Normalized single stage, radial compressor map (left) and normalized single stage radial expander map (right).

while achieving ultra-low emissions. This GT uses radial compressor and expander technology (without turbine blade cooling) that allows for more fuel flexibility, which is desirable for SOFC-GT hybrid systems. Single stage radial compressor [36] and expander [37] maps have been used to develop generalized maps as shown in Fig. 2.

The maps can be used for constant speed and variable speed operation. For variable speed operation it is necessary to adjust the frequency to the frequency of the grid, which is accomplished via a rectifier and inverter, each with a conversion efficiency of 98 %. When using VIGV the compressor map can be modified according to Equations (3)–(6) [38],

$$\dot{m}_{\text{Norm,Corr,VIGV}} = a \cdot \dot{m}_{\text{Norm,Corr}} \quad (3)$$

$$PR_{\text{Norm,Corr,VIGV}} = b \cdot PR_{\text{Norm,Corr}} \quad (4)$$

$$\eta_{\text{Norm,Corr,VIGV}} = c \cdot \eta_{\text{Norm,Corr}} \quad (5)$$

where

$$a, b, c = f(\Delta\alpha_{\text{VIGV}}) \quad (6)$$

The VIGV parameters a, b and c have been determined for $\Delta\alpha_{\text{VIGV}}$ ranging from 0 to 60° by curve-fitting data presented in [39]. The respective correlations are shown below.

$$a = -9.140 \cdot 10^{-5} \cdot \Delta\alpha_{\text{VIGV}}^2 + 1 \quad (7)$$

$$b = -8.178 \cdot 10^{-4} \cdot \Delta\alpha_{\text{VIGV}} + 1 \quad (8)$$

$$c = -3.804 \cdot 10^{-5} \cdot (\Delta\alpha_{\text{VIGV}} - 24.08)^2 + 1.022057 \quad (9)$$

The surge margin in this work is defined as the pressure ratio difference between the surge line and the operating point divided by the pressure ratio at the operating point at the corrected mass flow of the operating point.

$$SM = \frac{PR_{\text{surge}}(\dot{m}_{\text{Corr,OP}}) - PR_{\text{OP}}(\dot{m}_{\text{Corr,OP}})}{PR_{\text{OP}}(\dot{m}_{\text{Corr,OP}})} \quad (10)$$

Thermodynamically, the GT is modelled as compressor, combustor and expander whereby the design point performance input parameters such as polytropic efficiency, mechanical losses (incl. generator losses), heat loss and pressure drop are obtained from the on design point calibration case using vendor data [35]. In order to not exceed the maximum permissible blade metal temperature in the expander section of the GT, the following equation for the turbine inlet temperature (TIT) is employed [40].

$$TIT = TIT_R + \frac{644.23}{1.8} (y_{\text{H}_2\text{O}, \text{CO}_2\text{-R}} - y_{\text{H}_2\text{O}, \text{CO}_2}) \quad (11)$$

TIT is the turbine inlet temperature in degrees Celsius and $y_{\text{H}_2\text{O}, \text{CO}_2}$ is the mole fraction of H₂O plus CO₂ in the combustor outlet gas. The subscript R stands for the reference condition/design point. A summary of key GT operating parameters is provided in Table 2.

2.3. Economic analysis

Although SOFCs are highly modular, the majority of the hybrid plant is designed as single train. The plant configurations of the 10 MW SOFC-GT hybrid power plants investigated in this study consist of one fuel processing train designed for a plant capacity of 100 %, one GT and oxidizer at a capacity of 100 %, single train heat recuperation equipment at a capacity of 100 % and numerous pressurized SOFC modules at a capacity of $N \times 100/N\%$. Each of the SOFC modules consists of 22 stacks, each stack with its own ejector and pre-reformer. The 22 stacks are contained in one pressure vessel with thermal insulation.

The capital cost of the SOFC-GT plant equipment is established upon individual cost correlations [41] and supplier quotes. Heat exchangers have been sized and priced in a commercially available exchanger design software. The GT cost is calculated according to [35]. The SOFC stack cost, SOFC stack balance-of-plant equipment cost and power conditioning equipment cost are based upon work conducted by the Battelle Memorial Institute [42] for a factory production scale of 1000 modules per year (module size greater than 300 kW). The SOFC stack cost is comprised of 13 individual stack components/manufacturing steps: ceramic cell, end plates, interconnect, anode frame, picture frame, cathode frame, laser welding, ceramic-glass sealing, anode mesh, cathode mesh, stack assembly, stack brazing, and testing & conditioning. For details see [27,35]. Degradation of the SOFC stacks is accounted for in the form of spare stack installations and a 1st order degradation model of 0.2 % per 1000 h has been adopted. An SOFC lifespan of 10 years is assumed.

All equipment costs are escalated to a 2020-dollar basis using Equation (11) and an annual escalation rate of 3 %.

$$SC = RC \cdot (1 + AER)^{SY - RY} \quad (12)$$

RC is the reference cost, AER is the annual escalation rate, SY represents the scaled year and RY the respective reference year.

Expenses associated with the daily operation of the power plant, such as operating labor, maintenance materials & labor, administrative & support labor, consumables, fuel, and waste disposal are reported in the operating and maintenance costs.

Fixed operating costs consist of annual operating labor, maintenance

labor, administrative and support labor as well as property tax and insurance.

The plant is anticipated to be operated by 2 skilled workers on site who are paid 40.85 \$/h (escalated from [43]). Maintenance labor is estimated with 35 % of the maintenance cost. The maintenance costs themselves are established upon specific cost relationships [44]. The fuel used in this study is natural gas with a price of 3.96 \$/MMBtu [45]. In contrast to fuel, which is consumed, catalysts and sorbents are not directly used up but need to be replaced after a certain period of time due to deactivation. Thus, catalysts and sorbents are evaluated on their individual replacement rates. Furthermore, catalysts and sorbents require an initial fill before startup which contributes to the upfront costs. After reaching their end-of-life, those materials are disposed, which is associated with a disposal fee.

During the 1.5-year construction period the capital expenditure per half-year is: 10 %, 60 %, 30 %. One hundred percent of the total overnight capital is considered to be depreciable [46]. This financing structure can be approximated with a capital charge factor (CCF) of 0.0740. Using the above-described capital charge factor, the following equation can be used to calculate the first year's COE.

$$COE = \frac{(CCF)(TOC) + OC_{fix} + (CF)(OC_{var})}{(CF)(MWH)} \quad (13)$$

COE is the cost of electricity in the first year, CCF is the capital charge factor, TOC is the total overnight capital, OC_{fix} total fixed annual operating cost, OC_{var} total variable annual operating cost, CF the capacity factor of the plant and MWH is the annual net-megawatt hours generated at 100 % capacity factor.

3. Results and discussion

3.1. Operating conditions

A Dresser Rand KG2-3G EF GT has been selected in this work due to its fuel flexibility and rating at ISO conditions, which match with the desired GT size and operating conditions. Nevertheless, the differences between the KG2-3G EF and the custom-engineered GT in [18] require small modifications in the heat recuperation strategy. While it has been shown that using only the GT exhaust heat for pre-heating the SOFC air to 700 °C is favorable from an efficiency standpoint, the slightly higher pressure ratio of the KG2-3G EF makes it necessary to use additional heat

from the cathode off-gas for air pre-heating as shown in the flow sheet in Fig. 1.

When integrating a commercial GT designed for natural gas into an SOFC-GT hybrid, the operating point moves away from its natural gas design point. In an SOFC-GT hybrid, the fuel for the Brayton cycle is the unutilized fuel from the SOFC, which has a characteristically low heating value ranging from 1.09 MJ/kg to 1.74 MJ/kg (in this work), depending on the fuel utilization (high fuel utilization leads to a low heating value gas stream leaving the SOFC and vice versa). In this work, the FU is varied between a lower limit set by the heat integration of the pre-reformer, around 88 %, and an upper limit of around 92 % where the electrochemical reaction starts to severely slow down due to the reduced chemical potential difference. The anode off-gas is rich in H₂O and CO₂ leading to an increase in the H₂O and CO₂ concentrations in the gas stream entering the GT expander section when compared to natural gas. Due to the higher heat capacity of CO₂ and H₂O compared to diatomic gases, an adjustment of the TIT is required to maintain the same blade metal temperature as in the natural gas calibration case.

For constant speed operation, the maximum permissible firing temperatures (TIT_{MAX}) are: 909 °C (FU 88.2 %), 908 °C (FU 90.0 %) and 915 °C (FU 92.0 %), a substantial reduction when compared to the NG design point with a TIT of 943 °C. The changes in TIT_{MAX} are observed due to variations in the fuel to air ratio which is dictated by the SOFC. The higher the FU, the higher the SOFC cooling air requirement, which helps to decrease the concentrations of H₂O and CO₂ in the hot combustor outlet gas. A second effect impacting the air flow requirement is the SOFC operating pressure. Higher operating pressures increase the current density of the SOFC and thermal gradients, which results in a higher cathode air flow requirement in order to maintain the same thermal cell gradients. At constant speed operation, the 88.2 % FU scenario exhibits the highest operating pressure with a GT compressor discharge pressure of 7.77 bar. At a FU of 88.2 % sufficient quantities of fuel are left in the anode off-gas such that the maximum permissible TIT of 909 °C can be reached. In the 90.0 % FU scenario the TIT decreases 893 °C, which is 15 °C below the maximum permissible TIT. A further increase in FU exacerbates this effect and the 92.0 % FU scenario reaches a TIT of 809 °C, 106 °C lower than the maximum permissible TIT. The lower TIT and fuel to air ratio reduce the compressor discharge pressures to 7.72 bar in the 90.0 % FU scenario and 7.44 bar in the 92.0 % FU scenario, which is still above the design point pressure of 7.0 bar. The operating points are shown in Fig. 3.

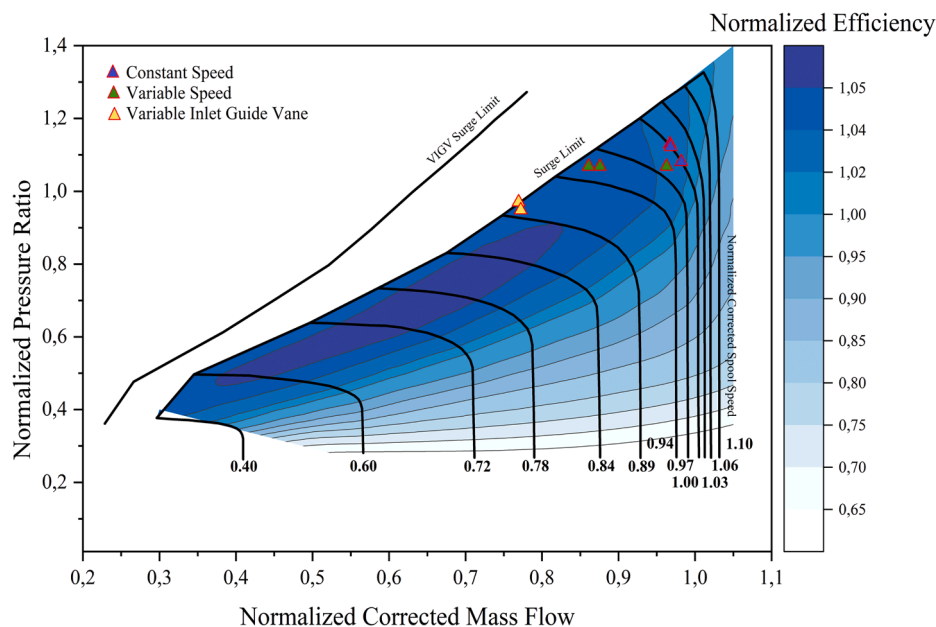


Fig. 3. SOFC-GT Hybrid operating points at off-design conditions.

The surge margin at the design point is 31.0 %, which reduces to 18.7 % for the 92.0 % FU scenario and to 11.7 % for the 88.2 % FU scenario as shown in Fig. 4.

For variable speed control the degrees of freedom of the system increase as the operating speed is not fixed. Thus, it is desirable to choose an operating condition that avoids concerns related to the surge margin. However, even at variable speed, the operating range of the GT is limited by the compressor and expander mismatch as well as the TIT. A compressor discharge pressure of 7.35 bar has been chosen as it is the lowest feasible discharge pressure to accommodate the three FU scenarios. At constant pressure, pressure effects related to the cooling air requirement of the SOFC are eliminated. Thus, the maximum permissible TIT_{MAX} or air cooling requirement is only dependent on the SOFC's FU. The lowest FU scenario with 88.8 % FU needs the least cooling air flow in the SOFC and thus, results in the lowest maximum permissible TIT_{MAX} of 908 °C. The 90.0 % FU scenario arrives at a TIT_{MAX} of 909 °C and the 91.9 % scenario allows a TIT_{MAX} of up to 915 °C. While the TIT_{MAX} is achievable in the 88.8 % FU scenarios, the higher FU scenarios cannot reach their respective TIT_{MAX} and operate at 889 °C (90.0 % FU) and 803 °C (91.9 % FU). As the FU decreases the operating point moves away from the design point horizontally towards the surge line. From Fig. 4 it becomes apparent how drastically the surge margin is reduced. For the 88.8 % FU scenario, surge margin reduces to 3.2 %. The 91.9 % FU scenario has a substantially higher surge margin (17.5 %); however, this value is still lower than the surge margin in the constant speed operation case at similar FU.

Under VIGV operation the compressor map changes which leads to a left shift of the surge limit. The GT still operates at constant speed but also the constant speed lines are shifted. This ultimately leads to a reduction in air mass flow and a lower compressor discharge pressure. Under a VIGV closing angle of 50°, the 87.6 %, 90.0 % and 91.9 % FU scenarios reach a compressor discharge pressure of 6.67 bar, 6.67 bar and 6.53 bar. The lower operating pressure allows the 87.6 % and 90.0 % FU scenarios to operate at their respective TIT_{MAX} of 907 °C and 910 °C. Just the higher fuel utilization scenario of 91.9 % FU operates at a TIT of 858 °C despite the fact that temperatures up to 917 °C are permissible. Closing the inlet guide vanes has a positive impact on the surge margin and the design point surge margin of 31.0 % can be almost maintained in the lower FU scenarios. The 91.9 % FU scenario even exceeds the design point surge margin, as seen in Fig. 4.

3.2. Hybrid thermodynamic performance

The GT power output ranges from 1.41 MW to 0.49 MW which is substantially lower than the GT's ISO rating of 1.83 MW. The GT power output is influenced by the GT efficiency and the mass flow rates. The GT

efficiency then again is affected by the compressor and expander efficiencies (off-design operation) as well as the TIT. As previously discussed, the TIT in these SOFC-GT hybrid applications decreases compared to the ISO rating, due to the higher concentration of H₂O and CO₂ in the combustor outlet gas stream as well as challenges with the heat integration. The mass flow rates on the other hand are reduced at higher pressure ratios, lower spool speeds and partially closed inlet guide vanes. Lower mass flows ultimately lead to less working fluid and less power generation. The compounding effect of all these factors can lead to a substantial GT derating.

The constant speed scenarios have the highest GT power output, as shown in Fig. 5. In Fig. 3, it can be seen that the constant speed operation results in the largest compressor air flow. When comparing the different FU scenarios within the constant speed scenario, it may be noticed that the GT power output decreases with increasing FU. In general, lower FUs lead to higher TITs resulting in higher GT efficiencies and higher GT power outputs. The effects of changes in pressure ratio and fuel to air ratio, which increases the mass flow through the GT expander, are rather small and do not significantly impact the overall GT power output in the constant speed scenarios. Changes in compressor and turbine efficiencies for the constant speed and VIGV scenarios are relatively small, too.

In the variable speed scenarios, pressure effects have been completely eliminated. The GT efficiency, impacted by the TIT and component efficiencies, and mass flow rate are the dominating factors determining the GT power output. Although a substantially higher mass flow in the variable speed, 91.9 % FU scenario is obtained and the compressor operates in a region of higher efficiency, it cannot fully compensate for the power loss associated with the temperature decrease of the TIT. At variable speed operation, lower FUs lead to lower mass flow rates as less air is needed to maintain a constant pressure level.

Closing the VIGVs has a similar effect on the compressor as reducing the speed. By controlling the flow cross section, air flow into the compressor is restricted resulting in lower air mass flow rates. The degree to which variable speed control or VIGVs are adapted can be freely specified in real world applications, in this work rather extreme cases are studied to identify the effectiveness of these measures. Under these circumstances, closing the VIGVs by 50° results in a flow reduction of more than 23 %, leading to the lowest GT power outputs among the studied scenarios. The GT power output trends within the VIGV operating mode follow the FU as discussed before.

The SOFC power output is strongly coupled to the FU and fuel to air ratio, since the operating voltage is held constant in all cases. The higher the FU, the more fuel is electrochemically converted in the SOFC increasing the power output. However, the GT air flow rate and the fuel to air ratio determine how many SOFCs can be used when paired with this specific GT. In an SOFC, the cooling air needed to maintain the same

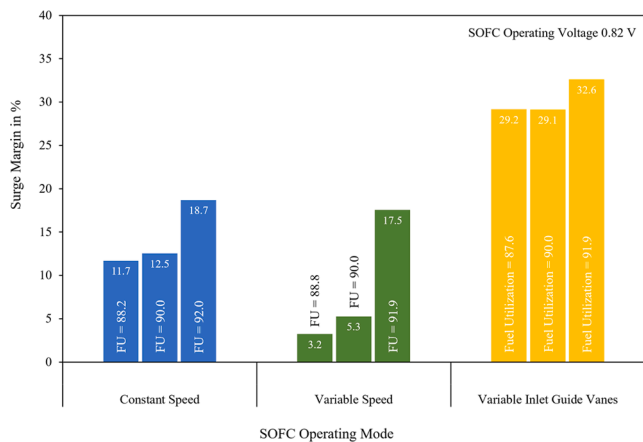


Fig. 4. Surge margins of SOFC-GT hybrid plant at respective off-design operating point.

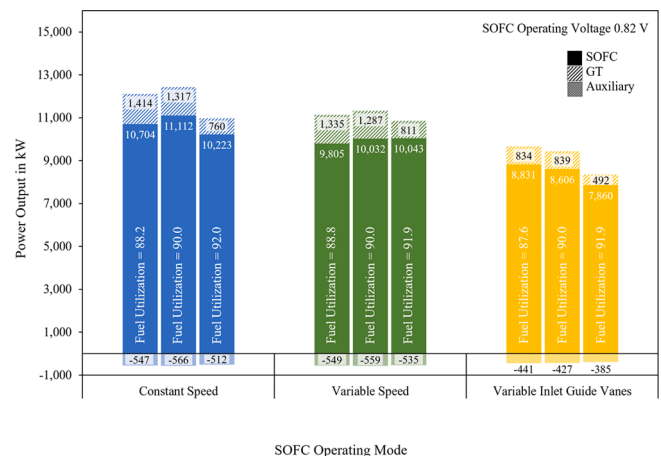


Fig. 5. Power generation and auxiliary load of SOFC-GT hybrid plants.

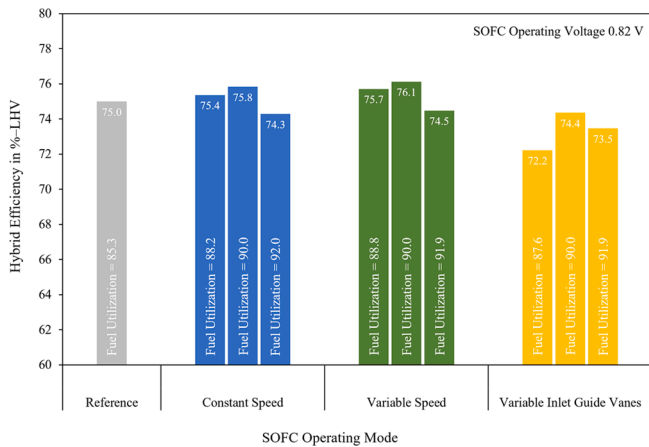


Fig. 6. Efficiency of SOFC-GT hybrid plants with off-the-shelf GT and reference case with custom-engineered GT.

thermal gradients is dependent on the operating condition. In general, the cooling air requirement is increased when higher operating pressures and/or higher FU factors are used. In fact, the cooling requirement increases drastically when operating the SOFC beyond 90 % FU. Since the air flow rate is set by the GT, the fuel flow and respectively the size of the SOFC are adjusted so that the air provided by the GT is sufficient for the amount of SOFCs installed. Thus, while a higher FU leads to more fuel being converted to electricity, it also leads to a down scaling of the SOFC due to the increased cooling requirement. Additionally, the GT air flow rate determines how many SOFCs can be accommodated. The balancing of these effects leads to the results shown in Fig. 5.

The efficiency of the hybrid plant is mostly influenced by the FU and the GT operating point. In an SOFC the voltage can be interpreted as a measure of efficiency; however, since the voltage in this study is held constant, only the SOFC's FU has an impact on the plant efficiency. An increase in the FU shifts power generation from the GT to the SOFC. SOFCs typically operate at a higher efficiency compared to GTs, leading to an overall increase in plant efficiency. Yet, if at the same time the GT operating point moves into a region of extremely low efficiency, the gains of shifting electricity generation from the GT to the SOFC might be diminished. This behavior can be seen at high FUs for all operating modes and is illustrated in Fig. 6.

When comparing the constant speed, variable speed and VIGV scenarios at a constant FU, differences between the different operating modes are mostly related to the GT. The impact of pressure ratio is small in that case and the TITs at constant FUs are similar across the different operating modes. Also, the effect of higher fuel to air ratio, which increases the mass flow through the GT expander but at the same time increases upstream fuel compression work, has only modest impact on the plant efficiency when comparing constant FUs.

Most of the efficiency gains in this constant FU comparison originate from the GT compressor and GT expander efficiency. While the GT operating points are relatively close within the constant speed, variable speed and VIGV scenarios, the operating points shift considerably between the aforementioned scenarios, as seen in Fig. 3. Such changes in GT component efficiencies can have a significant impact as GT compressor power consumption and GT expander power output are multiple times higher than the net power output of the GT. The highest efficiency is reached in the variable speed, 90.0 % FU scenario where the operating point of the GT is located in a region of high efficiency, as seen in Fig. 3. This high efficiency is reached despite the fact that variable speed control requires frequency adjustment which is associated with additional conversion losses in order to export the electricity to the grid. When comparing the efficiencies to the reference case with custom-engineered GT, the reference case does not exhibit the highest efficiency. The reason for this is that the reference case has been selected

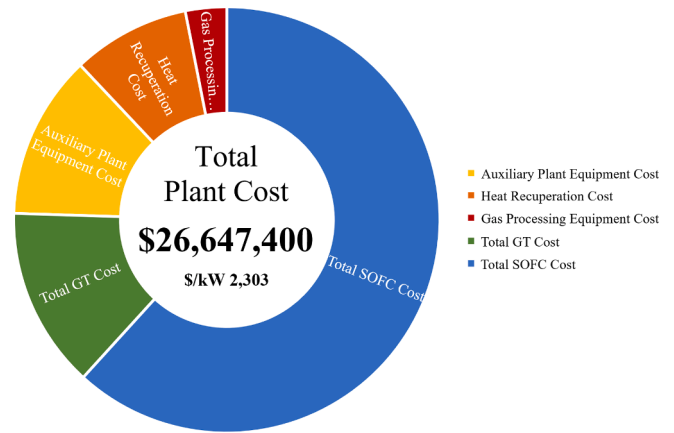


Fig. 7. SOFC-GT hybrid plant cost breakdown of the total plant cost (Const. Speed, 88.2% FU).

based upon the lowest COE and not the highest efficiency. In [18] higher efficiency cases have shown to be feasible, however, these ultra-high efficiency cases were less economical than the selected reference case.

3.3. Hybrid economics

In order to gauge a technology's competitiveness on the free market economic performance characteristics are needed to analyze tradeoffs between high efficiency, which reduces some operating costs, and capital cost over the plant's lifetime.

The total plant cost (TPC) is established based on the individual plant components and categorized into: SOFC cost, GT cost, auxiliary plant equipment cost, heat recuperation cost and gas processing cost. A characteristic breakdown of the TPC is shown in Fig. 7 using the constant speed, 88.2 % FU scenario as an example.

The SOFC cost constitutes the largest cost of the TPC with 61.8 %. This phenomenon is even more pronounced when moving to higher FU scenarios where the SOFC cost can be as high as 62.7 %. The GT represents the second most expensive TPC item. The GT is an off-the-shelf GT which is purchased at a fixed cost and the rest of the plant is scaled to match the GT. While the GT generates about 11.7 % of the

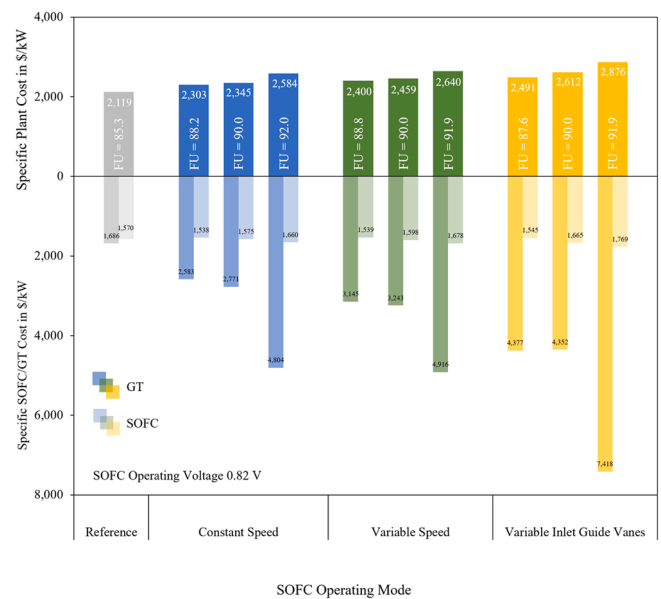


Fig. 8. Specific plant cost, specific SOFC cost and specific GT cost for SOFC-GT hybrid plants with off-the-shelf GT and reference case with custom-engineered GT.

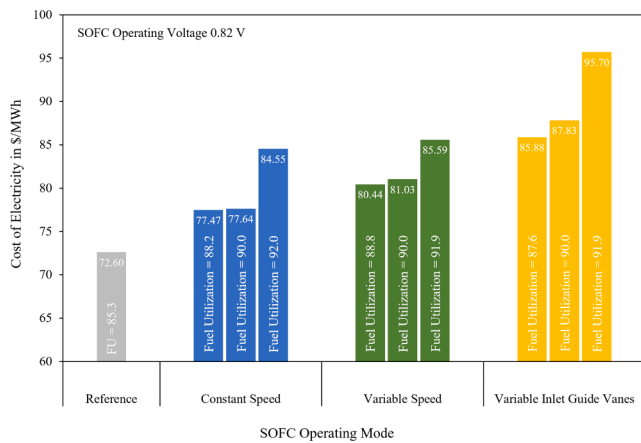


Fig. 9. Cost-of-electricity of SOFC-GT hybrid plants with off-the-shelf GT and reference case with custom-engineered GT.

electricity, it is responsible for 13.7 % of the TPC. Auxiliary plant equipment represents 12.4 %, heat recuperation 8.9 % and gas processing 3.1 % of the TPC.

Next, the specific plant costs as well as the specific cost for the two power-generating plant units are analyzed on a \$/kW basis as shown in Fig. 8. On the top of the zero-line, the specific plant cost is plotted. The specific GT costs and specific SOFC costs are mirrored at the zero-line. The specific SOFC cost remains fairly constant throughout the various scenarios. Low specific SOFC costs are achieved at low FUs. High FUs require over-proportionally more cell area at constant cell voltage as the chemical potential difference decreases. Other factors impacting the specific cell cost are the SOFC operating pressure. At the encountered

pressures, benefits associated with the increase in current density and reduction in cell area outweigh cost increases associated with the SOFC pressure vessel. Thus, for constant FUs, the lowest specific SOFC cost is obtained at the highest pressure ratio.

The specific GT cost exhibits a much wider range of fluctuations. As mentioned before, the GT is an off-the-shelf item that comes at a fixed cost. However, the variable speed operation requires frequency adjustment equipment since the electricity is not generated at grid frequency. Costs associated with frequency adjustment equipment are added to the GT cost in the variable speed scenarios. When correcting for this higher GT cost in the variable speed scenarios, the specific GT cost is directly related to the GT power output and follows the inverse trend of the GT power output as shown in Fig. 5.

The lowest specific plant costs are achieved in scenarios where low specific SOFC costs and low specific GT costs are obtained. The TPC and specific plant cost are also dependent on other equipment costs, however, gas processing equipment cost, heat recuperation equipment cost and auxiliary plant equipment cost remain relatively constant throughout the various scenarios and have no significant impact on the trend. Compared to the reference case with custom-designed GT it becomes clear that operating the hybrid not at its ideal conditions adds to the specific SOFC cost, specific GT cost and specific plant cost.

The specific plant cost is a strong indicator for the COE. Nevertheless, plant power output also plays an important role. Fixed costs like operating labor are tied to the number of operators present at the plant and the number of operators is based upon the plant's operating units. Since all plants in this study have the same number of operating units, the same number of operators are needed. Thus, variations of the net power output of the plant have an impact on the operating labor cost on a \$/MWh basis. Increasing the net plant power output decreases the relative labor cost.

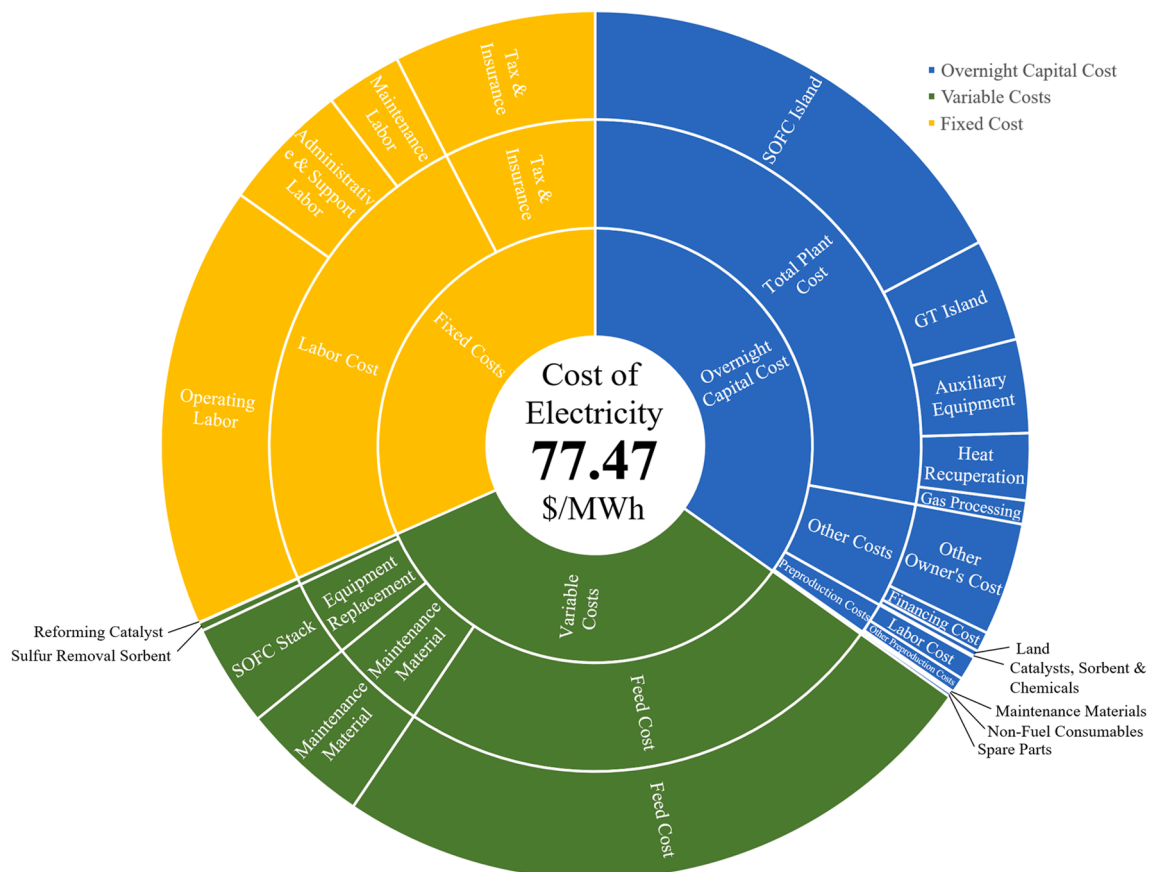


Fig. 10. SOFC-GT hybrid plant cost breakdown of the cost-of-electricity (Const. Speed, 88.2% FU).

All these effects are reflected in the COE and the lowest COEs are achieved for plants with high net power output and low specific plant cost. The lowest COE with 77.47 \$/MWh is reached in the constant speed, 88.2 % FU scenario which has the lowest specific plant cost and the second highest net power output. A slightly higher COE is obtained in the constant speed, 90.0 % FU scenario which has the second lowest specific plant cost and the highest net power output. Also from a purely technical point of view, a lower FU appears more attractive due to slightly lower thermal stress in the SOFC (considering the non-limiting thermal constrain parameter) and a higher heating value of the anode off-gas which is beneficial for maintaining stable oxidation. Compared to the reference case with custom-engineered GT the COE in the best-case scenario with off-the-shelf GT increased by 6.7 %. All COE results are summarized in Fig. 9.

In Fig. 10, a detailed breakdown of the different COE driving factors is shown for the constant speed, 88.2 % FU scenario. Overnight capital costs have the largest impact on the COE with a share of 34.8 % whereby the SOFC island alone is contributing 17.2 % to the COE. Variable costs have a share of 33.5 %. The by far largest variable cost is the fuel cost with 24.6 % despite the high fuel efficiency of the SOFC-GT hybrid plant. Maintenance material costs account for 4.8 % of the overall COE and the annual levelized SOFC stack replacement for 3.8 %. Fixed costs constitute 31.7 % of the COE. Operating labor is the dominant factor in the fixed costs with 16.5 %. Administrative & support labor account for 4.8 % and maintenance labor accounts for 2.9 %. Taxes & insurance represent 7.5 % of the COE.

4. Conclusion

An SOFC-GT hybrid system with off-the-shelf GT, as shown in Fig. 1, has been studied with respect to its thermodynamic and economic performance. Three different GT operating modes have been studied: I) constant spool speed operation, II) variable spool speed operation and III) partially closed compressor inlet guide vanes. For each GT operating mode, the performance was investigated over a range of SOFC fuel utilization factors, while considering physical constraints inside the SOFC, such as local temperature gradients in flow direction as well as overall cell temperature differences.

The results show that integrating an off-the-shelf GT into a SOFC-GT hybrid leads to a GT derating of 23–73 %. Major factors contributing to the GT derating are: I) a reduction in the TIT, II) a change of compressor and turbine efficiencies as the operating point shifts and III) effects of mass flow rate changes. Furthermore, the operating point of the gas turbine significantly impacts the SOFC operation, the main power producer in this SOFC-GT hybrid. To maximize the SOFC power output it is desirable operate the GT in a region of high air mass flow rates and low pressure ratios, which increases the number of stacks that can be accommodated and reduces the SOFC cooling requirement. Operating the system at constant spool speed has shown to lead to the highest net power output, with a net generation between 10.5 MW and 11.9 MW. Variable speed control reached the highest efficiency with 76.1 % LHV and VIGV control was able to provide the largest surge margin with 32.6 %. The surge margin is a major concern when operating the GT at constant speed or variable speed without VIGV control. Especially operating the SOFC at low FU factors, which leads to high TITs, is concerning with respect to the surge margin. In general, FUs of around 90 % are shown to have the highest efficiency.

The economic analysis revealed that the specific cost of the SOFC as well as the specific cost of the GT are reduced when operating the hybrid at low FU factors. The substantial derating of the GT power output has major implications not just for the economics of the GT but for the entire plant. When comparing the lowest-cost hybrid system with off-the-shelf GT to a hybrid system with a custom-engineered GT, an increase in the COE of 6.7 % is seen.

CRedit authorship contribution statement

Fabian Rosner: Conceptualization, Methodology, Software, Formal analysis, Investigation, Writing – original draft, Writing – review & editing. **Scott Samuelsen:** Writing – review & editing, Supervision, Project administration.

Declaration of Competing Interest

The authors declare that they have no known competing financial interests or personal relationships that could have appeared to influence the work reported in this paper.

Data availability

No data was used for the research described in the article.

Acknowledgements

The authors wish to acknowledge DOE's U.S. - China "Clean Energy Research Center for Water and Energy Technologies" program under whose sponsorship this work was conducted by the University of California, Irvine. Neither the U.S. Government nor any agency thereof, nor any of their employees, makes any warranty, express or implied, or assumes any legal liability or responsibility for the accuracy, completeness, or usefulness of any information, apparatus, product, or process disclosed, or represents that its use would not infringe privately owned rights. Reference herein to any specific commercial product, process, or service by trade name, trademark, manufacturer, or otherwise does not necessarily constitute or imply its endorsement, recommendation, or favoring by the U.S. Government or any agency thereof. The views and opinions of authors expressed herein do not necessarily state or reflect those of the U.S. Government or any agency thereof.

References

- [1] Yi Y, Rao AD, Brouwer J, Samuelsen GS. Analysis and optimization of a solid oxide fuel cell and intercooled gas turbine (SOFC-ICGT) hybrid cycle. *J Power Sources* 2004;132(1–2):77–85. <https://doi.org/10.1016/j.jpowsour.2003.08.035>.
- [2] Campanari S, Mastropasqua L, Gazzani M, Chiesa P, Romano MC. Predicting the ultimate potential of natural gas SOFC power cycles with CO₂ capture – Part B: applications. *J Power Sources* 2016;325:194–208. <https://doi.org/10.1016/j.jpowsour.2016.05.104>.
- [3] Massardo AF, Lubelli F. Internal reforming solid oxide fuel cell-gas turbine combined cycles (IRSOFC-GT): Part A—cell model and cycle thermodynamic analysis. *J Eng Gas Turbines Power* 2000;122(1):27. <https://doi.org/10.1115/1.483187>.
- [4] Kuchonthara P, Bhattacharya S, Tsutsumi A. Combinations of solid oxide fuel cell and several enhanced gas turbine cycles. *J Power Sources* 2003;124(1):65–75. [https://doi.org/10.1016/S0378-7753\(03\)00740-7](https://doi.org/10.1016/S0378-7753(03)00740-7).
- [5] Chan SH, Ho HK, Tian Y. Modelling of simple hybrid solid oxide fuel cell and gas turbine power plant. *J Power Sources* 2002;109(1):111–20. [https://doi.org/10.1016/S0378-7753\(02\)00051-4](https://doi.org/10.1016/S0378-7753(02)00051-4).
- [6] Chan SH, Ho HK, Tian Y. Multi-level modeling of SOFC-gas turbine hybrid system. *Int J Hydrogen Energy* 2003;28(8):889–900. [https://doi.org/10.1016/S0360-3199\(02\)00160-X](https://doi.org/10.1016/S0360-3199(02)00160-X).
- [7] Calise F, Dentice M, Palombo A, Vanoli L. Simulation and exergy analysis of a hybrid Solid Oxide Fuel Cell (SOFC)– Gas Turbine System. *Energy* 2006;31:3278–99. <https://doi.org/10.1016/j.energy.2006.03.006>.
- [8] Haseli Y, Dincer I, Naterer GF. Thermodynamic analysis of a combined gas turbine power system with a solid oxide fuel cell through exergy. *Thermochim Acta* 2008;480:1–9. <https://doi.org/10.1016/j.tca.2008.09.007>.
- [9] Eisavi B, Chitsaz A, Hosseinpour J, Ranjbar F. Thermo-environmental and economic comparison of three different arrangements of solid oxide fuel cell-gas turbine (SOFC-GT) hybrid systems. *Energy Convers Manag* 2018;168(January):343–56. <https://doi.org/10.1016/j.enconman.2018.04.088>.
- [10] Arsalis A. Thermo-economic modeling and parametric study of hybrid SOFC-gas turbine-steam turbine power plants ranging from 1.5 to 10 MWe. *J Power Sources* 2008;181(2):313–26. <https://doi.org/10.1016/j.jpowsour.2007.11.104>.
- [11] Wongchanapai S, Iwai H, Saito M, Yoshida H. Performance evaluation of a direct-biogas solid oxide fuel cell-micro gas turbine (SOFC-MGT) hybrid combined heat and power (CHP) system. *J Power Sources* 2013;223:9–17. <https://doi.org/10.1016/j.jpowsour.2012.09.037>.

- [12] Uechi H, Kimijima S, Kasagi N. Cycle analysis of gas turbine-fuel cell cycle hybrid micro generation system. *J Eng Gas Turbines Power* 2004;126(4):755. <https://doi.org/10.1115/1.1787505>.
- [13] Yang WJ, Park SK, Kim TS, Kim JH, Sohn JL, Ro ST. Design performance analysis of pressurized solid oxide fuel cell/gas turbine hybrid systems considering temperature constraints. *J Power Sources* 2006;160(1):462–73. <https://doi.org/10.1016/j.jpowsour.2006.01.018>.
- [14] Cuneo A, Zaccaria V, Tucker D, Sorce A. Gas turbine size optimization in a hybrid system considering SOFC degradation. *Appl Energy* 2018;230(March):855–64. <https://doi.org/10.1016/j.apenergy.2018.09.027>.
- [15] Zhang L, Li X, Jiang J, Li S, Yang J, Li J. Dynamic modeling and analysis of a 5-kW solid oxide fuel cell system from the perspectives of cooperative control of thermal safety and high efficiency. *Int J Hydrogen Energy* 2015;40(1):456–76. <https://doi.org/10.1016/j.ijhydene.2014.10.149>.
- [16] Wu X, Yang D, Wang J, Li X. Temperature gradient control of a solid oxide fuel cell stack. *J Power Sources* 2019;414:345–53. <https://doi.org/10.1016/j.jpowsour.2018.12.058>.
- [17] Shirazi A, Aminyavari M, Najafi B, Rinaldi F, Razaghi M. Thermal-economic-environmental analysis and multi-objective optimization of an internal-reforming solid oxide fuel cell-gas turbine hybrid system. *Int J Hydrogen Energy* 2012;37(24):19111–24. <https://doi.org/10.1016/j.ijhydene.2012.09.143>.
- [18] Rosner F, Rao A, Samuelsen S. Thermo-economic analyses of solid oxide fuel cell-gas turbine hybrids considering thermal cell gradients. *J Power Sources* 2021;507:230271. <https://doi.org/10.1016/j.jpowsour.2021.230271>.
- [19] Rosner F, Yang D, Rao A, Samuelsen S. Gas turbine price projection for n-th plant equipment cost. *Eng Econ* 2022;67(1):1–6. <https://doi.org/10.1080/0013791X.2022.2048330>.
- [20] Lundberg WL, Veyo SE, Moeckel MD. A high-efficiency sofc hybrid power system using the mercury 50 ats gas turbine. In: *Proceedings of ASME TURBO EXPO 2001 June 4-7, 2001, New Orleans, Louisiana, 2001*, pp. 1–8, doi: 10.1115/2001-GT0521.
- [21] Park SK, Oh KS, Kim TS. Analysis of the design of a pressurized SOFC hybrid system using a fixed gas turbine design. *J Power Sources* 2007;170(1):130–9. <https://doi.org/10.1016/j.jpowsour.2007.03.067>.
- [22] Costamagna P, Magistri L, a. F. Massardo. Design and part-load performance of a hybrid system based on a solid oxide fuel cell reactor and a micro gas turbine. *J Power Sources* 2001;96(2):352–68. [https://doi.org/10.1016/S0378-7753\(00\)00668-6](https://doi.org/10.1016/S0378-7753(00)00668-6).
- [23] Barelli L, Bidini G, Ottaviano A. Part load operation of SOFC/GT hybrid systems: Stationary analysis. *Int J Hydrogen Energy* 2012;37(21):16140–50. <https://doi.org/10.1016/j.ijhydene.2012.08.015>.
- [24] Kimijima S, Kagsagi N. Performance evaluation of gas turbine-fuel cell hybrid micro generation system; 2002.
- [25] Calise F, Palombo A, Vanoli L. Design and partial load exergy analysis of hybrid SOFC-GT power plant. *J Power Sources* 2006;158(1):225–44. <https://doi.org/10.1016/j.jpowsour.2005.07.088>.
- [26] Campanari S. Full load and part-load performance prediction for integrated SOFC and microturbine systems. *J Eng Gas Turbines Power* 2000;vol. 122, no. April:239. <https://doi.org/10.1115/99-GT-065>.
- [27] Rosner F, Rao A, Samuelsen S. Economics of cell design and thermal management in solid oxide fuel cells under SOFC-GT hybrid operating conditions. *Energy Convers Manag Sep.* 2020;220:112952. <https://doi.org/10.1016/j.enconman.2020.112952>.
- [28] U.S. Department of Energy/NETL. Quality Guidelines For Energy System Studies; Specification for Selected Feedstocks, DOE/NETL-341/011812, 2012.
- [29] Union Gas, Chemical Composition of Natural. <https://www.uniongas.com/about-us/about-natural-gas/chemical-composition-of-natural-gas> (accessed Aug. 30, 2019).
- [30] Colton JW. Pinpoint Carbon Deposition. *Hydrocarb Process* 1981.
- [31] Fuel Cell Energy. Development of a Microchannel High Temperature Recuperator for Fuel Cell Systems. DOE Grant No. DE-EE0001111; 2014.
- [32] Zhu Y, Cai W, Wen C, Li Y. Fuel ejector design and simulation model for anodic recirculation SOFC system. *J Power Sources* 2007;173(1):437–49. <https://doi.org/10.1016/j.jpowsour.2007.08.036>.
- [33] Khandkar AC, Elangovan S, Hartvigsen J. Integrated reformer/CPN SOFC stack module design; 1995.
- [34] Li M, Powers JD, Brouwer J. A finite volume SOFC model for coal-based integrated gasification fuel cell systems analysis. *J Fuel Cell Sci Technol* 2010;7(4):0410171–04101712. <https://doi.org/10.1115/1.4000687>.
- [35] “2019 GTW Handbook,” *Gas Turbine World*, vol. 34, 2019.
- [36] Radial Compressor Test Case. Numeca Int. Announc. Press; 1999.
- [37] Pullen KR, Baines NC, Hill SH. The design and evaluation of a high pressure ratio radial turbine. *ASME 1992 Int. Gas Turbine Aeroengine Congr. Expo. GT 1992*, vol. 1, pp. 1–7, 1992, doi: 10.1115/92-GT-093.
- [38] Kim TS, Hwang SH. Part load performance analysis of recuperated gas turbines considering engine configuration and operation strategy. *Energy* 2006;31(2–3):260–77. <https://doi.org/10.1016/j.energy.2005.01.014>.
- [39] Ishino M, Pnakiri Y, Bessho A, Uchida H. Effects of variable inlet guide vanes on small centrifugal compressor performance. *Int. Gas Turbine Aeroengine Congr. Exhibition Indianapolis, Indiana; 1999*.
- [40] Rosner F, Chen Q, Rao A, Samuelsen S, Jayaraman A, Alptekin G. Process and economic data on the thermo-economic analyses of IGCC power plants employing warm gas CO₂ separation technology. *Data Br Dec.* 2019;27(104716):104716. <https://doi.org/10.1016/j.dib.2019.104716>.
- [41] Woods DR. Rules of thumb in engineering practice; 2007.
- [42] Battelle Memorial Institute. Manufacturing cost analysis of 100 and 250 kW fuel cell systems for primary power and combined heat and power applications. DOE Contract No. DE-EE0005250; 2016.
- [43] U.S. Department of Energy/NETL. Cost and performance baseline for fossil energy plants volume 1: Bituminous coal and natural gas to electricity. NETL-PUB-22638; 2019.
- [44] U.S. Department of Energy/NETL. Cost and performance baseline for fossil energy plants volume 3a: Low rank coal to electricity: IGCC cases. DOE/NETL-2010/1399; 2011.
- [45] “Short-Term Energy Outlook - January 2019,” U.S. Energy Inf. Adm.
- [46] U.S. Department of Energy/NETL. Quality guidelines for energy system studies; cost estimation methodology for NETL assessments of power plant performance, NETL-PUB-22580, 2019, [Online]. Available: http://www.netl.doe.gov/FileLibrary/research/energy_analysis/publications/QGESSNETLCostEstMethod.pdf.